Synthesis and Spectroscopic Characterization of $(CO)_6Fe_2\{\mu\text{-}EC(H){=}C(H)E'\}$ ($E \neq E'$; E, E′ = S, Se, Te) and $(CO)_6Fe_2\{\mu\text{-}TeC(H){=}C(H)Te\}$. Structural Characterization of $(CO)_6Fe_2\{\mu\text{-}SC(Ph){=}C(H)Se\}$ and $(CO)_6Fe_2\{\mu\text{-}SC(H){=}C(Ph)Te\}$

Pradeep Mathur,* Aswini K. Dash, Md. Munkir Hossain, and
Shubhangi B. Umbarkar

Department of Chemistry, Indian Institute of Technology, Powai, Bombay 400 076, India

C. V. V. Satyanarayana

*Regional Sophisticated Instrumentation Center, Indian Institute of Technology, Powai,
Bombay 400 076, India*

Yu-Sheng Chen, Elizabeth M. Holt, S. Narasinga Rao, and Manuel Soriano

University of Central Oklahoma, 100 N. University Drive, Edmond, Oklahoma 73034-0175

Received October 16, 1996[⊗]

When acetylene gas was bubbled through methanol solutions containing the mixed-chalcogenide compounds $(CO)_6Fe_2(\mu\text{-}EE')$ ($E \neq E'$; E, E′ = S, Se, Te), the acetylene adducts $(CO)_6Fe_2\{\mu\text{-}EC(H){=}C(H)E'\}$ (**1**, 52%, E, E′ = S, Se; **2**, 46%, E, E′ = S, Te; **3**, 38%, E, E′ = Se, Te) were obtained. In addition, trace amounts of the homochalcogenide derivatives $(CO)_6Fe_2\{\mu\text{-}EC(H){=}C(H)E\}$ (E = S, Se, Te) were also obtained. The Te_2 compound $(CO)_6Fe_2\{\mu\text{-}TeC(H){=}C(H)Te\}$ (**4**) was obtained in 32% yield from the reaction of $(CO)_6Fe_2(\mu\text{-}Te_2)$ with acetylene. Compounds **1**−**4** were characterized by IR and ^1H, ^{13}C, ^{77}Se, and ^{125}Te NMR spectroscopy. Crystallographic analysis of the phenylacetylene adducts $(CO)_6Fe_2\{\mu\text{-}SC(Ph){=}C(H)Se\}$ (**5**) and $(CO)_6Fe_2\{\mu\text{-}SC(H){=}C(Ph)Te\}$ (**6**) were carried out. The structures of both **5** and **6** can be described as Fe_2SE (E = Se, Te) tetrahedral butterfly cores containing the phenylacetylene as a bridge between the two wingtip chalcogen atoms, with three terminally bonded carbonyl groups on each Fe atom.

Introduction

Acetylene activation on transition-metal complexes is of considerable importance, because the reduction of acetylenes to olefins is an important probe of the active metallic center in the enzyme nitrogenase[1] and because there is interest in transforming the coordinated alkynes into useful organic species.[2] Although there exist a large number of reports on the different types of bonding modes of acetylenes to transition metals,[3] investigations on activation of acetylenes on main group elements are more recent and far fewer. The utility of the class of compounds $(CO)_6Fe_2(\mu\text{-}E_2)$ (E = S, Se, Te) for facile synthesis of mixed-metal clusters and for additions of small organic moieties has been demonstrated.[4] In both types of reactions, the bridging chalcogen atoms are the sites of addition, and the reactivities of $(CO)_6Fe_2(\mu\text{-}E_2)$ compounds are found to depend on the nature of E ligands. For instance, $(CO)_6Fe_2(\mu\text{-}Te_2)$ reacts at room temperature with $W(CO)_5(THF)$ to form the mixed-metal cluster $WFe_2(CO)_{10}(\mu_3\text{-}Te_2)$ but shows no reactivity toward $Mo(CO)_5(THF)$.[5] On the other hand, $(CO)_6Fe_2(\mu\text{-}Se_2)$ reacts with both the W and Mo carbonyl compounds to form the clusters $MFe_2(CO)_{10}(\mu_3\text{-}Se_2)$ (M = Mo, W). Similarly, whereas $(CO)_6Fe_2(\mu\text{-}Se_2)$ can add phenylacetylene across its Se-Se bond to form $(CO)_6Fe_2\{\mu\text{-}SeC(H){=}C(Ph)Se\}$,[6] both $(CO)_6Fe_2(\mu\text{-}S_2)$ and $(CO)_6Fe_2(\mu\text{-}Te_2)$ are inert toward phenylacetylene addition. We have earlier reported the convenient synthesis of the mixed-chalcogenide compounds $(CO)_6Fe_2(\mu\text{-}EE')$[4c,7] (E, E′ = S, Se, Te), and their reactivity toward phenylacetylene has been studied.[8] In a continuation of our investigation on the reactions of the $(CO)_6Fe_2(\mu\text{-}EE')$ compounds toward organic species, we report here on the reaction of acetylene with $(CO)_6Fe_2(\mu\text{-}SSe)$, $(CO)_6Fe_2(\mu\text{-}STe)$, $(CO)_6Fe_2(\mu\text{-}SeTe)$, and $(CO)_6Fe_2(\mu\text{-}Te_2)$. Crystal structures of the phenylacetylene derivatives $(CO)_6Fe_2\{\mu\text{-}SC(Ph){=}C(H)Se\}$ and $(CO)_6Fe_2\{\mu\text{-}SC(H){=}C(Ph)Te\}$ are also reported.

[⊗] Abstract published in *Advance ACS Abstracts,* February 1, 1996.

(1) Pombeiro, A. J. L.; Richards, R. L. *Coord. Chem. Rev.* **1990**, *104*, 13.

(2) Katz, T. J.; Hacker, S. M. *J. Am. Chem. Soc.* **1985**, *107*, 2182.

(3) (a) Deeming, A. J. *Adv. Organomet. Chem.* **1986**, *26*, 1. (b) Vargas, M. D.; Nicholas, J. N. *Adv. Inorg. Chem. Radiochem.* **1986**, *30*, 126. (c) Braga, D.; Grepioni, F.; Johnson, B. F. G.; Lewis, J.; Lunniss, J. A. *J. Chem. Soc., Dalton Trans.* **1992**, 1101. (d) Bonnemann, H. *Angew. Chem., Int. Ed. Engl.* **1985**, *24*, 248. (e) Sappa, E.; Tiripicchio, A.; Braunstein, P. *Chem. Rev.* **1983**, *83*, 1081.

(4) (a) Mathur, P.; Chakrabarty, D.; Mavunkal, I. J. *J. Cluster Sci.* **1993**, *4*, 351. (b) Mathur, P.; Hossain, M. M.; Rheingold, A. L. *Organometallics* **1995**, *14*, 2115. (c) Mathur, P.; Sekar, P.; Satyanarayana, C. V. V.; Mahon, M. F. *Organometallics* **1995**, *14*, 2115.

(5) Mathur, P.; Chakrabarty, D.; Hossain, M. M.; Rashid, R. S.; Rugmini, V.; Rheingold, A. L. *Inorg. Chem.* **1992**, *31*, 1106.

(6) (a) Mathur, P.; Hossain, M. M. *Organometallics* **1993**, *12*, 2398. (b) Mathur, P.; Hossain, M. M.; Das, K.; Sinha, U. C. *J. Chem. Soc., Chem. Commun.* **1992**, 46.

(7) (a) Mathur, P.; Chakrabarty, D.; Hossain, M. M. *J. Organomet. Chem.* **1991**, *401*, 167. (b) Mathur, P.; Chakrabarty, D.; Hossain, M. M. *J. Organomet. Chem.* **1991**, *418*, 415

(8) Mathur, P.; Hossain, M. M.; Umbarkar, S.; Satyanarayana, C. V. V.; Tavale, S. S.; Puranik, V. G. *Organometallics* **1995**, *14*, 959.

Table 1. Conditions Used for Preparation of $(CO)_6Fe_2\{\mu\text{-}EC(H){=}C(H)E'\}$ ($E \neq E'$; E, E′ = S, Se, Te and E = E′ = Te)

compd	$Fe_2(CO)_6(\mu\text{-}EE')$ [amt, g (mmol)]	time, h	product	yield, g (%)	anal. found (calcd)	mp, °C
1	$Fe_2(CO)_6(\mu\text{-}SSe)$ [0.6 (1.53)]	18	$Fe_2(CO)_6\{\mu\text{-}SC(H){=}C(H)Se\}$	0.33 (52)	C, 23.3 (23.02); H, 0.52 (0.48)	94−96
2	$Fe_2(CO)_6(\mu\text{-}STe)$ [0.6 (1.36)]	30	$Fe_2(CO)_6\{\mu\text{-}SC(H){=}C(H)Te\}$	0.29 (46)	C, 20.72 (20.6); H, 0.52 (0.43)	100−102
3	$Fe_2(CO)_6(\mu\text{-}SeTe)$ [0.6 (1.23)]	36	$Fe_2(CO)_6\{\mu\text{-}SeC(H){=}C(H)Te\}$	0.24 (38)	C, 19.06 (18.71); H, 0.45 (0.39)	116−118
4	$Fe_2(CO)_6(\mu\text{-}Te)_2$ [0.6 (1.12)]	48	$Fe_2(CO)_6\{\mu\text{-}TeC(H){=}C(H)Te\}$	0.2 (32)	C, 17.47 (17.08); H, 0.46 (0.36)	122−124

Table 2. Crystallographic Data for 5 and 6

	5	6
formula	$C_{14}HFe_2O_6SSe$	$C_{14}HFe_2O_6STe$
fw	487.9	1078.2
cryst syst	monoclinic	triclinic
space group	$P2_1/c$	$P\bar{1}$
a, Å	17.974(2)	7.4914(9)
b, Å	6.822(10)	10.5901(18)
c, Å	14.008(2)	12.1323(8)
α, deg	90.0	105.533(7)
β, deg	97.070(10)	102.250(7)
γ, deg	90.0	106.553(15)
V, Å^3	1704.4(4)	876.6(2)
Z	4	2
D_{calc}, g cm^{-3}	1.901	1.23
hkl ranges	h, −23 to +23; k, −8 to +1; l, −1 to +18	h, 0−9; k, −12 to +10; l, −14 to +11
corrections	Lorentz−polarizn; semiempirical abs and extinction	Lorentz−polarizn; no abs or decay
convergence largest shift, Å	0.06	0.03
minimization factor	$\sum w(F_o - F_c)^2$	$\sum w\|F_o - kF_c\|^2$
least-squares weights	$w^{-1} = \sigma^2(F) + 0.0008F^2$	$4F_o^2/[\sigma(F_o)^2]^2$
total obsd reflections	1503	3250
R, %	5.29	5.4
R_w, %	6.65	6.8

Experimental Section

General Procedures. Reactions and manipulations were carried out under an inert atmosphere of nitrogen or argon using standard Schlenk techniques. Solvents were purified and deoxygenated immediately prior to use. Infrared spectra were recorded on a Nicolet Impact 400 Fourier transform spectrometer in NaCl cell of 0.1 mm path length as hexane solutions. ^1H, ^{13}C, ^{77}Se, and ^{125}Te NMR spectra were obtained on a Varian VXR-300S spectrometer in $CDCl_3$ solutions using appropriate references at 25 °C. The ^{77}Se NMR signals were referenced to Me_2Se ($\delta = 0$), and the spectra were obtained at an operating frequency of 57.23 MHz; 90° pulses were used with 2 s delay and 1 s acquisition time. ^{125}Te NMR measurements were made at an operating frequency of 94.705 MHz using a pulse of 90° and a delay of 1 s. The spectra were referenced to Me_2Te ($\delta = 0$). Elemental analyses were carried out using a Carlo Erba automatic analyzer. $(CO)_6Fe_2(\mu\text{-}EE')$[4c,7] ($E \neq E'$; E, E′ = S, Se, Te) and $(CO)_6Fe_2(\mu\text{-}Te_2)$ were prepared as reported in the literature.[9] Phenylacetylene was purchased from Aldrich Chemical Co. and used as such.

Typical Preparation of $(CO)_6Fe_2\{\mu\text{-}EC(H){=}C(H)E'\}$ ($E \neq E'$; E, E′= S, Se, Te and E = E′ = Te). Conditions used for preparation of **1**−**4** are summarized in Table 1. In a typical preparation, acetylene gas was bubbled, at a slow rate, with constant stirring at room temperature, into a methanol solution (15 mL) containing freshly prepared $(CO)_6Fe_2(\mu\text{-}EE')$ ($E \neq E'$; E, E′ = S, Se, Te and E = E′ = Te) and anhydrous sodium acetate (0.25 g). The reactions were monitored by TLC and terminated when all the $(CO)_6Fe_2(\mu\text{-}EE')$ had been consumed. The solution was filtered through Celite to remove insoluble material. After removal of the solvent, the residue was redissolved in 5 mL of hexane and subjected to chromatographic workup on a silica gel column. Using hexane as eluent, three closely spaced bands were collected; the major orange-red band of $(CO)_6Fe_2\{\mu\text{-}EC(H){=}C(H)E'\}$ was eluted as the second band in each case. The first and third bands were minor and were identified as the corresponding homochalcogenide compounds $(CO)_6Fe_2\{\mu\text{-}EC(H){=}C(H)E\}$ and $(CO)_6Fe_2\{\mu\text{-}E'C(H){=}C(H)E'\}$.

Table 3. Selected Bond Distances and Bond Angles for 5

Bond Distances (Å)			
S(1)−Fe(1)	2.289(3)	Se(1)−Fe(2)	2.385(2)
S(1)−Fe(2)	2.289(3)	Se(1)−Fe(1)	2.380(2)
S(1)−C(2)	1.808(13)	Se(1)−C(1)	1.929(13)
C(1)−C(2)	1.293(19)	Fe(1)−Fe(2)	2.501(3)
Bond Angles (deg)			
Fe(1)−S(1)−Fe(2)	66.2(1)	Fe(1)−Se(1)−Fe(2)	63.3(1)
S(1)−Fe(2)−Fe(1)	56.9(1)	Se(1)−Fe(1)−Fe(2)	58.4(1)
S(1)−Fe(2)−Se(1)	81.0(1)	Se(1)−Fe(1)−S(1)	81.1(1)
S(1)−Fe(1)−Fe(2)	56.9(1)	Se(1)−Fe(2)−Fe(1)	58.2(1)
S(1)−C(2)−C(1)	117.4(10)	Se(1)−C(1)−C(2)	118.1(10)

Crystal Structure Determination of $(CO)_6Fe_2\{\mu\text{-}SC(Ph){=}C(H)Se\}$ (5). A deep red needle-shaped crystal of approximate dimensions 0.2 × 0.2 × 0.3 mm^3 was selected and mounted on a goniometer. The data were collected on a Siemens R3m/V diffractometer employing Mo Kα ($\lambda = 0.710\,73$ Å) radiation at a temperature of 301 K using the $\omega{-}2\theta$ scan method. Pertinent crystallographic data are listed in Table 2. A total of 5099 reflections were collected, and 1503 reflections with $F_o > 7.0\sigma(F_o)$ were used in refinement using full-matrix lease-squares methods. The structure was solved by Siemens SHELXTL Plus (PC version) by direct methods. The hydrogen atoms were located in difference Fourier maps. The non-hydrogen atoms were refined anisotropically to a final R factor of 0.0529 for 242 variables. Table 3 lists the selected bond lengths and bond angles for **5**.

Crystal Structure Determination of $(CO)_6Fe_2\{\mu\text{-}SC(H){=}C(Ph)Te\}$ (6). A red, plate-shaped single crystal of approximate dimensions 0.14 × 0.36 × 0.42 mm^3 was mounted on a goniometer and placed on a Siemens P4 diffractrometer. The data were collected using Mo Kα ($\lambda = 0.71073$ Å) radiation at room temperature, using the $\omega{-}2\theta$ scan method.

Crystallographic data are summarized in Table 2. A total of 3355 reflections with $F_o > 3\sigma(F_o)$ were used in refinement.

---

[9] Bogan, L. E.; Lesch, D. A.; Rauchfuss, T. B. *J. Organomet. Chem.* **1983**, *250*, 429.

Table 4. Selected Bond Distances and Bond Angles for 6

Bond Distances (Å)			
S−Fe(1)	2.263(2)	Te−Fe(2)	2.545(1)
S−Fe(2)	2.269(2)	Te−Fe(1)	2.547(1)
S−C(7)	1.79(1)	Te−C(8)	2.526(2)
C(7)−C(8)	1.32(1)	Fe(1)−Fe(2)	2.526(2)
Bond Angles (deg)			
Fe(1)−S−Fe(2)	67.76(7)	Fe(1)−Te−Fe(2)	59.47(4)
S−Fe(1)−Fe(2)	56.23(7)	Te−Fe(2)−Fe(1)	60.30(4)
S−Fe(2)−Te	80.96(7)	Te−Fe(1)−S	81.03(7)
S−Fe(2)−Fe(1)	56.01(7)	Te−Fe(1)−Fe(2)	60.23(4)
S−C(7)−C(8)	122.4(7)	Te−C(8)−C(7)	112.3(7)
C(7)−C(8)−C(9)	128.4(7)	Te−C(8)−C(9)	119.4(4)

Scheme 1. Formation of $(CO)_6Fe_2\{\mu\text{-}EC(H){=}C(H)E'\}$ (E ≠ E′; E, E′ = S, Se, Te and E = E′ = Te)

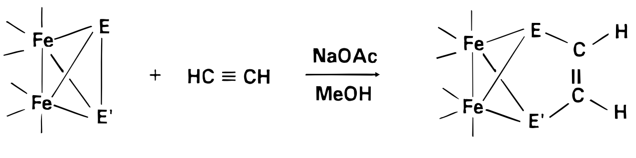

	E	E′
1.	S	Se
2.	S	Te
3.	Se	Te
4.	Te	Te

The structure was solved by SHELX using direct methods, and the hydrogen atoms were located in the Fourier difference maps. The non-hydrogen atoms were refined anisotropically, and the hydrogen atoms were refined isotropically by full-matrix least square techniques to a final *R* factor of 0.054 for 235 variables. Table 4 lists the selected bond lengths and bond angles for **6**.

Results and Discussion

Synthesis. When acetylene gas was bubbled through a methanol solution of mixed-chalcogenide compounds $(CO)_6Fe_2(\mu\text{-}SSe)$, $(CO)_6Fe_2(\mu\text{-}STe)$, and $(CO)_6Fe_2(\mu\text{-}SeTe)$ in the presence of sodium acetate, the acetylene adducts $(CO)_6Fe_2\{\mu\text{-}SC(H){=}C(H)Se\}$ (**1**; 52%), $(CO)_6Fe_2\{\mu\text{-}SC(H){=}C(H)Te\}$ (**2**; 46%), and $(CO)_6Fe_2\{\mu\text{-}SeC(H){=}C(H)Te\}$ (**3**; 38%) were obtained, respectively (Scheme 1). In each case, small amounts of the corresponding homochalcogenide derivatives $(CO)_6Fe_2\{\mu\text{-}EC(H){=}C(H)E\}$ (E = S, Se, Te) were also isolated. No other products were obtained in these reactions. The identity of $(CO)_6Fe_2\{\mu\text{-}SC(H){=}C(H)S\}$[10] and $(CO)_6Fe_2\{\mu\text{-}SeC(H){=}C(H)Se\}$[11] was confirmed by comparison of their IR spectra with those reported earlier. The new Te_2 compound $(CO)_6Fe_2\{\mu\text{-}TeC(H){=}C(H)Te\}$ (**4**) could also be obtained in 32% yield when acetylene gas was bubbled through a methanol solution of $(CO)_6Fe_2(\mu\text{-}Te_2)$, in the presence of sodium acetate. The exact role of sodium acetate in these and the earlier reported reactions is not known. When the above reactions were performed in the absence of sodium acetate, much lower yields of products were obtained. Attempts to obtain the known compound $(CO)_6Fe_2\{\mu\text{-}SC(H){=}C(H)S\}$ by the method of bubbling acetylene through a basic methanolic solution of $(CO)_6Fe_2(\mu\text{-}S_2)$ yielded only a trace amount of the product. Seyferth has obtained this compound in good yield from the reaction of HC≡CMgBr with $(CO)_6Fe_2(\mu\text{-}S)_2$ followed by protonation with CF_3CO_2H.[10]

The compounds $(CO)_6Fe_2(\mu\text{-}EE')$ are known to decompose in solution, and it is possible that $Fe(CO)_x$ fragments liberated may influence the reactivity of acetylene toward these compounds. The rates of their decomposition vary depending on the E, E′ combinations; $(CO)_6Fe_2(\mu\text{-}SSe)$ is the most unstable and thus provides $Fe(CO)_x$ fragments most readily and should facilitate the addition of acetylene to the undecomposed $(CO)_6Fe_2(\mu\text{-}SSe)$ faster than with other $(CO)_6Fe_2(\mu\text{-}EE')$ species, as observed. The involvement of $Fe(CO)_x$ fragments in these reactions is probably only one of several factors contributing to the difference in reactivity observed. The nature of the R group in RC≡CH is important in controlling the addition of the acetylenic triple bond across the E−E′ bond. Whereas acetylene readily adds to $(CO)_6Fe_2(\mu\text{-}Te_2)$, phenylacetylene is inert toward such additions. However, under thermolytic conditions, $(CO)_9Fe_3(\mu_3\text{-}Te_2)$ reacts with phenylacetylene to form $(CO)_6Fe_2\{\mu\text{-}TeC(H){=}C(Ph)Te\}$.[12] Probably, the $Fe(CO)_3$ fragments formed as a result of fragmentation of $(CO)_9Fe_3(\mu_3\text{-}Te_2)$ under reaction conditions effect the addition of phenylacetylene to $(CO)_6Fe_2(\mu\text{-}Te_2)$, formed in situ.

Spectroscopic Characterization. Infrared and ^1H, ^{13}C, ^{77}Se, and ^{125}Te NMR data for **1**−**4** are given in Table 5. The IR spectra of the four compounds exhibit identical CO stretching patterns, typically observed for compounds containing $Fe_2(CO)_6$ groups. Comparison of these spectra with the earlier reported ones for $(CO)_6Fe_2\{\mu\text{-}SC(H){=}C(H)S\}$ and $(CO)_6Fe_2\{\mu\text{-}SeC(H){=}C(H)Se\}$ shows that there is a regular lowering of the corresponding ν(CO) frequencies along the following combinations of the chalcogen ligands: $S_2 > SSe > Se_2 > STe > SeTe > Te_2$. The ^1H NMR spectra of compounds **1**−**3** show two doublets for the nonequivalent CH protons and satellites due to coupling with ^{77}Se and ^{125}Te isotopes. In **1**, the upfield signal, at δ 6.79 ppm, shows an H−Se coupling of 8 Hz, which is comparable to the three-bond H−Se coupling of 9.2 Hz in $(CO)_6Fe_2\{\mu\text{-}TeC(H){=}C(Ph)Se\}$ reported earlier, and therefore this signal can be assigned to SC*H*. The downfield signal at δ 6.94 ppm shows a much larger H−Se coupling of 50 Hz, which is comparable with the two-bond coupling of 50.4 Hz observed in $(CO)_6Fe_2\{\mu\text{-}SeC(H){=}C(Ph)S\}$ and therefore can be assigned to SeC*H*. Similarly, the assignments for **2** and **3** have been made and it is seen that the more downfield signal is due to the CH which is attached to the more electropositive chalcogen. The ^1H NMR spectrum of **4** shows a single peak with satellites corresponding to short-range and long-range couplings, which are comparable with those reported for $(CO)_6Fe_2\{\mu\text{-}TeC(H){=}C(Ph)Te\}$. The $^{13}C(^1H)$ NMR spectra of **1**−**3** show two signals, each one split into a doublet of doublets due to short-range and long-range C−H coupling. Moreover, in **1** the signal at δ 136 ppm also shows C−Se coupling (94 Hz), and therefore it may be assigned to Se*C*. Similarly, in the spectrum of **3**, the signal at δ 148 ppm shows C−Se coupling (104 Hz) and, therefore, this signal can be assigned to Se*C*. The spectrum of **4** shows a doublet of doublets with C−H coupling within

---

(10) Seyferth, D.; Womack, G. B. *Organometallics* **1986**, *5*, 2360.

(11) Mathur, P.; Dash, A. K.; Hossain, M. M.; Satyanarayana, C. V. V. *J. Organomet. Chem.* **1995**, *493*, 257.

(12) Fassler, T.; Buchholz, D.; Huttner, G.; Zsolnai, L. *J. Organomet. Chem.* **1989**, *369*, 297.

Table 5. Spectroscopic Data for 1−4

compd	IR (cm^{-1}, hexane)	^{1}H NMR (δ, CDCl$_3$)	^{13}C{^{1}H} NMR (δ, CDCl$_3$)	^{77}Se NMR (δ, CDCl$_3$)	^{125}Te NMR (δ, CDCl$_3$)
 $\mathrm{S{-}C(H){=}C(H){-}Se}$ **1**	2077 (s), 2041 (vs), 2004 (m), 1992 (m)	6.79 (SC*H*; d, J_{H-H} = 4.8 Hz, J_{H-Se} = 8 Hz), 6.94 (SeC*H*; d, J_{H-H} = 4.8 Hz, J_{H-Se} = 50 Hz)	136 (Se*C*H; dd, J_{C-H} = 9.1, 189 Hz, J_{C-Se} = 94 Hz), 146 (S*C*H; dd, J_{C-H} = 9.1, 185 Hz), 208 (*C*O)	306 (dd, $^3J_{Se-H}$ = 8 Hz, $^2J_{Se-H}$ = 50 Hz)	
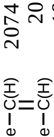 $\mathrm{Se{-}C(H){=}C(H){-}Se}$	2074 (vs), 2039 (s), 2001 (vs), 1987 (m), 1965 (m)	7.43 (SeC*H*; $^3J_{H-Se}$ = 10 Hz, $^2J_{H-Se}$ = 54 Hz)	138 (Se*C*H; dd, J_{C-H} = 9, 188 Hz, J_{C-Se} = 98 Hz), 209 (*C*O)	383 (dd, $^3J_{Se-H}$ = 10 Hz, $^2J_{Se-H}$ = 54 Hz)	
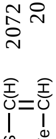 $\mathrm{S{-}C(H){=}C(H){-}Te}$ **2**	2072 (m), 2036 (vs), 2002 (m), 1997 (m)	7.43 (SC*H*; d, J_{H-H} = 5.4 Hz, $^3J_{H-Te}$ = 6 Hz) 7.59 (TeC*H*; d, J_{H-H} = 5.4 Hz, $^2J_{H-Te}$ = 106 Hz)	116 (Te*C*H; dd, J_{C-H} = 6.8, 187 Hz), 155 (S*C*H; dd, J_{C-H} = 6.8, 183 Hz), 209 (*C*O)		536 (dd, $^3J_{Te-H}$ = 6 Hz, $^2J_{Te-H}$ = 106 Hz)
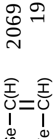 $\mathrm{Se{-}C(H){=}C(H){-}Te}$ **3**	2069 (vs), 2033 (s), 1997 (m), 1986 (m)	8.02 (SeC*H*; d, J_{H-H} = 5.1 Hz, $^2J_{H-Se}$ = 60 Hz, $^3J_{H-Te}$ = 13 Hz), 8.41 (TeC*H*; d, J_{H-H} = 5.1 Hz, $^2J_{H-Te}$ = 119 Hz, $^3J_{H-Se}$ = 13 Hz)	118 (Te*C*H; dd, J_{C-H} = 7, 184 Hz), 148 (Se*C*H; dd, J_{C-H} = 7, 185 Hz, J_{C-Se} = 104 Hz), 210 (*C*O)	456 (dd, $^3J_{Se-H}$ = 13 Hz, $^2J_{Se-H}$ = 60 Hz)	680 (dd, $^3J_{Te-H}$ = 15 Hz, $^2J_{Te-H}$ = 119 Hz)
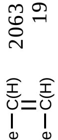 $\mathrm{Te{-}C(H){=}C(H){-}Te}$ **4**	2063 (s), 2028 (vs), 1992 (s), 1978 (m)	9.23 (TeC*H*; s, $^3J_{H-Te}$ = 20.5 Hz, $^2J_{H-Te}$ = 132.5 Hz)	131 (Te*C*H; dd, J_{C-H} = 7.2, 185 Hz), 211 (*C*O)		806 (dd, $^3J_{Te-H}$ = 21 Hz, $^2J_{Te-H}$ = 133 Hz)

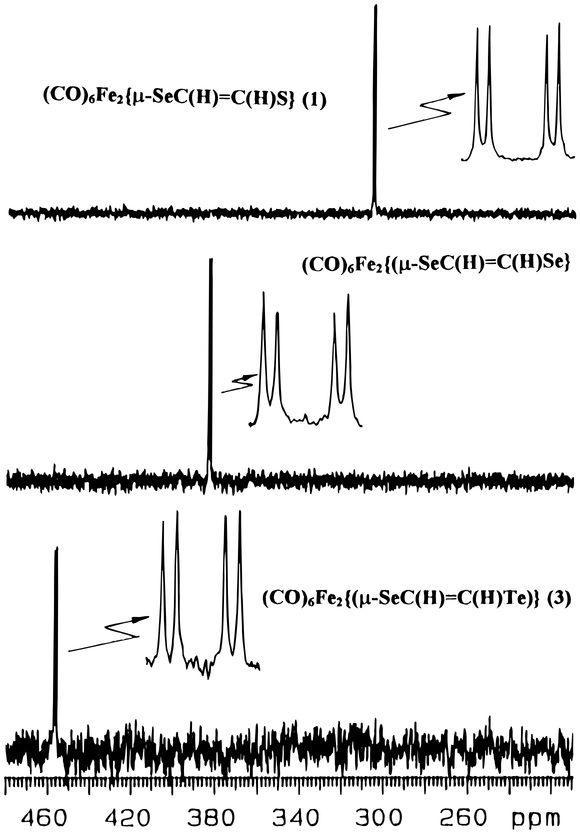

Figure 1. ^{77}Se NMR spectra.

the range observed for **1**−**3**. A single peak between δ 208 and 211 ppm for the CO ligands is observed in the spectra of all four compounds, indicating that the carbonyl ligands are equivalent on the NMR time scale at room temperature. ^{77}Se NMR spectra of **1** and **3** each show a doublet of doublets due to short-range and long-range Se−H coupling (Figure 1). The chemical shifts, δ 306 and 456 ppm, respectively, are in the range of chemical shifts of previously reported compounds: δ 383 ppm for $(CO)_6Fe_2\{\mu\text{-}SeC(H){=}C(H)Se\}$,[11] δ 303 ppm for $(CO)_6Fe_2\{\mu\text{-}SeC(H){=}C(Ph)S\}$, δ 371 and 448 ppm for $(CO)_6Fe_2\{\mu\text{-}SeC(H){=}C(Ph)Se\}$, and δ 436 ppm for $(CO)_6Fe_2\{\mu\text{-}SeC(H){=}C(Ph)Te\}$.[8] Similarly, the ^{125}Te NMR spectra of **2**−**4** showed doublets of doublets at δ 536, 680, and 806 ppm, respectively (Figure 2). These are in the range of chemical shifts observed in the following compounds: δ 533 ppm in $(CO)_6Fe_2\{\mu\text{-}SC(Ph){=}C(H)Te\}$, δ 658 ppm in $(CO)_6Fe_2\{\mu\text{-}SeC(Ph){=}C(H)Te\}$, and δ 769 and 931 pppm in $(CO)_6Fe_2\{\mu\text{-}TeC(Ph){=}C(H)Te\}$.[8] The short-range and long-range Se−H coupling constants in $(CO)_6Fe_2\{\mu\text{-}SeC(H){=}C(H)E\}$ (E = S, Se, Te) increase along the series E = S, Se, Te. Likewise, the short-range and long-range Te−H couplings show a similar trend for the compounds $(CO)_6Fe_2\{\mu\text{-}TeC(H){=}C(H)E\}$ (E = S, Se, Te). Similar trends of increasing J_{Se-H} and J_{Te-H} values were observed in the series of compounds $(CO)_6Fe_2\{\mu\text{-}SeC(H){=}C(Ph)E\}$ and $(CO)_6Fe_2\{\mu\text{-}TeC(H){=}C(Ph)E\}$ (E= S, Se, Te), respectively.

Molecular Structure of $(CO)_6Fe_2\{\mu\text{-}SC(Ph){=}C(H)Se\}$ (5). The phenylacetylene adduct $(CO)_6Fe_2\{\mu\text{-}SC(Ph){=}C(H)Se\}$ (**5**) was prepared as reported earlier.[8] Deep red air-stable crystals of **5** were obtained from a hexane/CH_2Cl_2 solution at −10 °C, and an X-ray diffraction study was undertaken. An ORTEP diagram of the molecular structure of **5** is shown in Figure 3. The

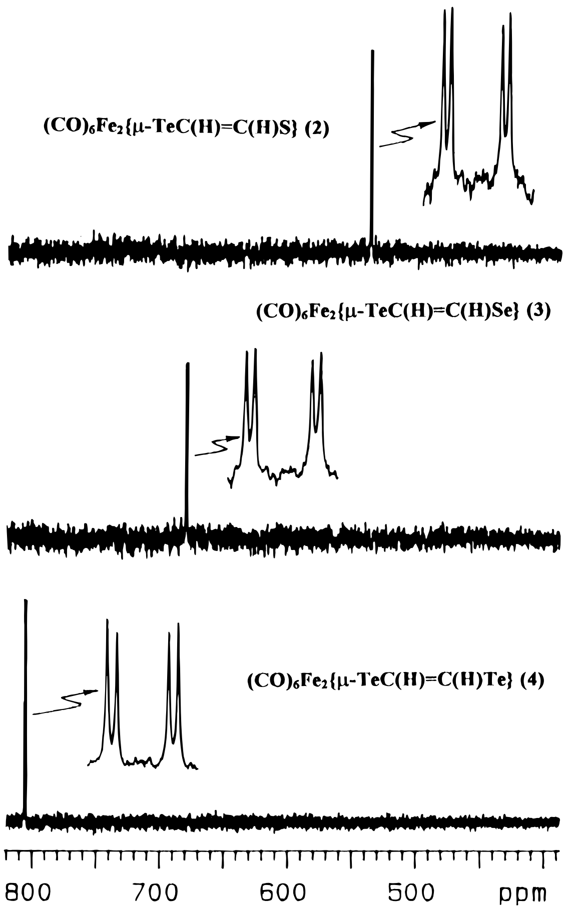

Figure 2. ^{125}Te NMR spectra.

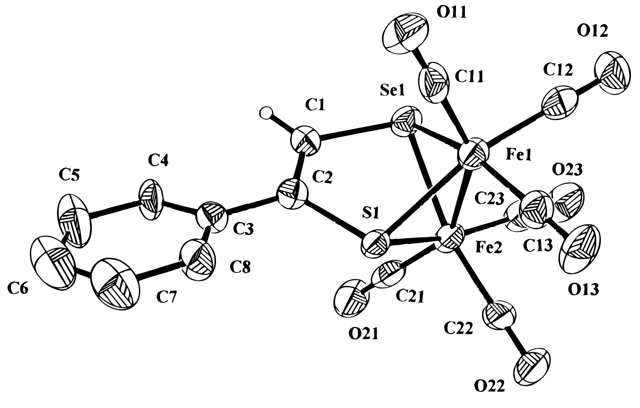

Figure 3. Molecular structure of **5** with thermal ellipsoids at the 50% probability level.

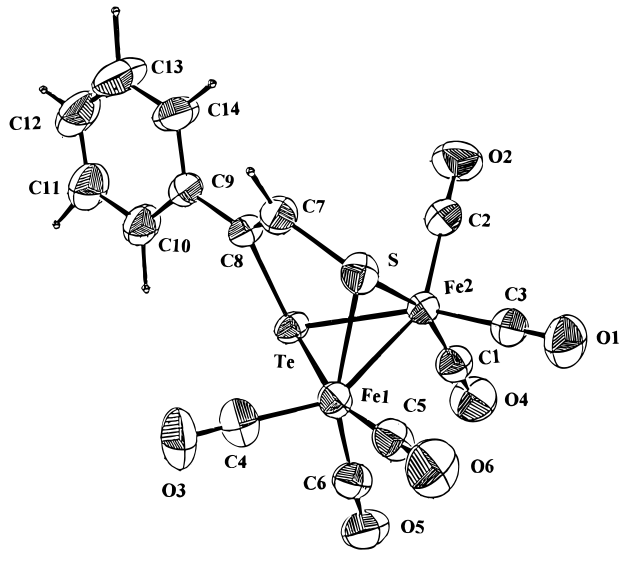

Figure 4. Molecular structure of **6** with thermal ellipsoids at the 50% probability level.

structure consists of an Fe_2SSe butterfly core, and the phenylacetylene molecule is attached to the wingtip S and Se atoms of the butterfly, such that the CH group is bonded to the Se atom and the CPh group to the S atom. Each Fe atom has three terminally bonded carbonyl groups. The three CO groups, the μ_3-S ligand, μ_3-Se ligand, and the Fe−Fe bond define a distorted-octahedral geometry around each Fe atom. Overall the structure of **5** is similar to those of $(CO)_6Fe_2\{\mu\text{-SeC(H)=C(Ph)Se}\}$, $(CO)_6Fe_2\{\mu\text{-SeC(H)=C(Ph)Te}\}$, and $(CO)_6Fe_2\{\mu\text{-TeC(H)=C(Ph)Te}\}$. The C(1)−C(2) bond distance of 1.293(13) Å indicates reduction of the acetylene triple bond to an olefinic bond. It is similar to the corresponding bond distance of coordinated acetylene bonds in $(CO)_6Fe_2\{\mu\text{-SeC(H)=C(Ph)Se}\}$ (1.331(7) Å) and $(CO)_6Fe_2\{\mu\text{-SeC(H)=C(Ph)Te}\}$ (1.31(3) Å). The Fe−Fe bond distance of 2.501(3) Å in **5** is somewhat shorter than in the related compounds $(CO)_6Fe_2(\mu\text{-Se}_2)$ (2.552(2) Å),[13] $(CO)_6Fe_2(\mu\text{-S}_2)$ (2.575(2) Å),[14] $(CO)_6Fe_2\{\mu\text{-SeC(H)=C(Ph)Se}\}$ (2.512(1) Å),[11] $(CO)_6Fe_2\{\mu\text{-SeC(H)=C(Ph)Te}\}$ (2.539(5) Å),[8] and $(CO)_6Fe_2\{\mu\text{-TeC(H)=C(Ph)Te}\}$ (2.571(4)Å).[12] The C−Se bond distance of 1.929(13) Å in **5** compares well with the C−Se bond distances in $(CO)_6Fe_2\{\mu\text{-SeC(H)=C(Ph)Se}\}$ (1.917(5) Å) and $(CO)_6Fe_2\{\mu\text{-SeC(H)=C(Ph)Te}\}$ (1.92(2) Å). The average Se−Fe−S angle of 81° in **5** is similar to the average Se−Fe−Se angle of 81.4° in $(CO)_6Fe_2\{\mu\text{-SeC(Ph)=C(H)Se}\}$ but greater than the average S−Fe−S angle of 53.6° in $(CO)_6Fe_2(\mu\text{-S})_2$ and Se-Fe-Se angle of 58° in $(CO)_6Fe_2(\mu\text{-Se})_2$, consistent with an almost equal amount of opening of the Fe_2SSe and the Fe_2Se_2 butterfly cores to accommodate the phenylacetylene molecule.

Molecular Structure of $(CO)_6Fe_2\{\mu\text{-SC(H)=C(Ph)Te}\}$ (6). The phenylacetylene adduct $(CO)_6Fe_2\{\mu\text{-SC(H)=C(Ph)Te}\}$ (**6**) was prepared as reported earlier.[8] Red plate-shaped air-stable crystals of **6** were grown from its hexane/CH_2Cl_2 solutions at −10 °C, and an X-ray analysis was undertaken. Figure 4 shows the molecular structure of **6**. Phenylacetylene is bonded to the wingtips of the Fe_2STe butterfly tetrahedral core geometry such that the CH and CPh groups are attached to the S and Te atoms, respectively. The acetylenic bond distance C(7)−C(8), at 1.32(1) Å, is similar to the corresponding bond distance of 1.31(3) Å in $(CO)_6Fe_2\{\mu\text{-SeC(H)=C(Ph)Te}\}$ and 1.31(1) Å in $(CO)_6Fe_2\{\mu\text{-TeC(H)=C(C≡CCH}_3\text{)S}\}$ but shorter than in $(CO)_6Fe_2\{\mu\text{-TeC(H)=C(Ph)Te}\}$ (1.34(1) Å). Overall, the structure is similar to that of **5**. The Fe−Fe bond distance of 2.526(2) Å in **6** is shorter than the corresponding distance of 2.571(4) Å in $(CO)_6Fe_2\{\mu\text{-TeC(H)=C(Ph)Te}\}$ but comparable to those in other related Te-containing acetylenic derivatives: $(CO)_6Fe_2\{\mu\text{-TeC(H)=C(C≡CCH}_3\text{)S}\}$ (2.5328(2) Å) and $(CO)_6Fe_2\{\mu\text{-SeC(H)=C(Ph)Te}\}$ (2.539(5) Å). The Fe−Te bond length in $(CO)_6Fe_2\{\mu\text{-SC(H)=C(Ph)Te}\}$ is 2.546(1) Å, similar to those in $(CO)_6Fe_2\{\mu\text{-SeC(H)=C(Ph)Te}\}$ (average 2.5405 Å) and $(CO)_6Fe_2\{\mu\text{-TeC(H)=C(C≡CCH}_3\text{)S}\}$ (average 2.5422 Å) but longer than

---

[13] Campana, C. F.; Lo, F. W.-K.; Dahl, L. F. *Inorg. Chem.* **1979**, *18*, 3060.

[14] Wei, C. H.; Dahl, L. F. *Inorg. Chem.* **1965**, *4*, 1.

the average Fe−Te bond distance of 2.525 Å in $(CO)_6Fe_2\{\mu\text{-}TeC(H){=}C(Ph)Te\}$. The Fe−Te−Fe bond angle of 59.47(4)° in **6** is smaller than the Fe−S−Fe bond angle of 67.76(7)° but similar to the corresponding bond angles in $(CO)_6Fe_2\{\mu\text{-}SeC(H){=}C(Ph)Te\}$ (59.95(13)°) and in $(CO)_6Fe_2\{\mu\text{-}TeC(H){=}C(Ph)Te\}$ (61.3(1) and 61.2(1)°).

Investigations are currently in progress to examine the reactivities of different $RC{\equiv}CR'$ species toward $(CO)_6Fe_2(\mu\text{-}EE')$ and also the possibilities of the catalytic role of reactive metal carbonyl species in the reaction solutions.

Acknowledgment. We thank the Council of Scientific & Industrial Research, Government of India, for financial support.

Supporting Information Available: Complete tables of atomic coordinates, bond lengths, bond angles, and anisotropic thermal parameters for **5** and **6** (10 pages). Ordering information is given on any current masthead page.

OM950815U